JOURNAL OF GEOPHYSICAL RESEARCH, VOL. 106, NO. A4, PAGES 6195–6201, APRIL 1, 2001

Latitudinal density dependence of magnetic field lines inferred from Polar plasma wave data

J. Goldstein,[1] R. E. Denton, M. K. Hudson, E. G. Miftakhova, and S. L. Young

Department of Physics and Astronomy, Dartmouth College, Hanover, New Hampshire

J. D. Menietti

Department of Physics and Astronomy, University of Iowa, Iowa City, Iowa

D. L. Gallagher

NASA Marshall Space Flight Center, Huntsville, Alabama

Abstract. Using observations of the electron density n_e based on measurement of the upper hybrid resonance frequency by the Polar spacecraft Plasma Wave Instrument, we have examined the radial density dependence along field lines in the outer plasmasphere and the near plasma trough. Our technique depends on the fact that Polar crosses particular L values at two different points with different radial distance R. Sampled L values range from 2.5 to 6.3. In our plasmaspheric data set ($n_e \geq 100$ cm^{-3}) we find that, on average, n_e is flat along field lines from the equator up to the latitudes sampled by Polar ($R \gtrsim 2\ R_E$). In the plasma trough data set ($n_e < 100$ cm^{-3}) there is, on average, a mild radial dependence $n_e \propto R^{-1.7}$.

1. Introduction

While the average properties of the equatorial plasma density in the magnetosphere have been relatively well described [*Carpenter and Anderson*, 1992; *Gallagher et al.*, 2000], there have been few studies of the latitudinal density dependence along field lines. Results from the DE 1 spacecraft indicate that the normal situation is for the electron density n_e to be fairly constant along field lines both in the outer plasmasphere ($L \gtrsim 3$) and in the plasma trough (at least for altitudes well above the ionosphere so that $R \gtrsim 2\ R_E$, where R is the radial distance from the Earth's center and R_E is the radius of the Earth) [*Décréau et al.*, 1986; *Olsen et al.*, 1987; *Olsen*, 1992; *Gallagher et al.*, 2000]. At the equator, density minima [*Décréau et al.*, 1986; *Olsen et al.*, 1987; *Olsen*, 1992] and maxima [*Gallagher et al.*, 2000] are sometimes observed, but observations of these are relatively rare. The equatorial minima and maxima are possibly associated with the refilling of depleted flux tubes [*Gallagher et al.*, 2000], though refilling structures have never been unambiguously identified. Considerable work has been performed in the analysis of flux tube filling, including hydrodynamic and kinetic modeling, which is well discussed by *Lemaire and Gringauz* [1998]. The nearly constant density observed by DE 1 is consistent with the constant density predicted for a completely trapped population in a dipole field [*Chan et al.*, 1994] and is also roughly consistent with a diffusive equilibrium solution [e.g., *Young et al.*, 1980].

In an earlier study, *Angerami and Carpenter* [1966] used ground-based whistler wave data to infer a field line density dependence consistent with diffusive equilibrium (nearly constant) in the plasmasphere, but $n_e \propto R^{-4}$ in the plasma trough. This last result is the so-called "collisionless" dependence resulting from an exospheric equilibrium with no equatorially trapped particles (consistent with a Maxwellian at the top of the collisional region near the surface of the Earth) [*Lemaire and Gringauz*, 1998, and references therein]. While their plasmaspheric results agree with the DE 1 studies, the steep R^{-4} plasma trough dependence was not verified by those studies. Angerami and Carpenter's results, however, depended on the extrapolation of the radial dependence down to an altitude of 1000 km (altitude of the Alouette 1 satellite). It may be possible to reconcile the data of Angerami and Carpenter with the DE 1 results by coupling a steep ionospheric density dependence at low altitudes with a nearly constant density at high altitudes [*Gallagher et al.*, 2000].

[1]Now at Department of Physics and Astronomy, Rice University, Houston, Texas

Paper number 2000JA000068.
0148-0227/01/2000JA000068$09.00

Yet another technique is to infer mass density ρ_m using toroidal (azimuthal) Alfvén wave frequencies [*Menk et al.*, 1999, and references therein]. Using observations of such waves at geosynchronous orbit ($L = 6.6$), *Takahashi and McPherron* [1982] inferred the radial dependence of mass density ranging from constant density along field lines to $\rho_m \propto R^{-4}$. *Menk et al.* [1999] found the radial dependence to vary between R^{-1} and R^{-6} at $L = 2.8$ and 3.7. At these L values, the inferred radial dependencies are characteristic of the outer parts of the field lines (near the equator) and do not represent the much steeper dependence in the vicinity of the ionosphere. It must be kept in mind that these measurements are for mass density, not electron density; small fractional densities of oxygen can significantly affect ρ_m. However, at values of $L \gtrsim 3$ the mass density on the bulk of the field lines is normally expected to be hydrogen dominated [*Poulter et al.*, 1988; *Craven et al.*, 1997]. Further tests of these techniques using comparison with spacecraft data would be beneficial. At low latitudes, where the ionosphere is relatively more important ($L \lesssim 2.4$), a very strong variation of mass density along field lines is expected [*Poulter et al.*, 1988; *Price et al.*, 1999].

During one period of its lifetime, the DE 1 spacecraft had a polar orbit with apogee at nearly 0° magnetic latitude [see *Décréau et al.*, 1986, Figure 1]. This orbit is useful for studying the variation in density along magnetic field lines in the vicinity of the equator, since the shape of the orbit is close to (but not exactly) that of a magnetic field line in that region. On the other hand, the finite variation in L along the orbit introduces a significant uncertainty because the density dependence across L shell is greater than that along a field line. Correction factors may be applied to factor out the L dependence, but these depend on an assumption for the L dependence (like density $\propto L^{-4}$ as in the works of *Décréau et al.* [1986] and *Olsen* [1992]).

The Polar spacecraft orbit, illustrated in Figure 1 (sketch at top), leads to a different possibility for studying the density dependence along field lines. In Figure 1 the perigee of the orbit is at point 4. The Polar spacecraft makes two passes through the plasmasphere (shaded regions to the left and right of the Earth labeled "I" and "II"), one approaching perigee (I, with points 1–3), and one leaving perigee (II). The largest electron density n_e values in Figure 1 occur while the spacecraft is in the plasmasphere. The lowest L value occurs at point 2. Measurements on the data segment between points 1 and 2 can be paired with measurements on the data segment between points 2 and 3 such that the paired points have the same L shell. On the other hand, these points will have differing radial distance from the center of the Earth R, as the bottom panel in Figure 1 demonstrates. Because of this, we can infer the field line variation of density on the L shell containing two such points. For example, consider the points 1 and 3.

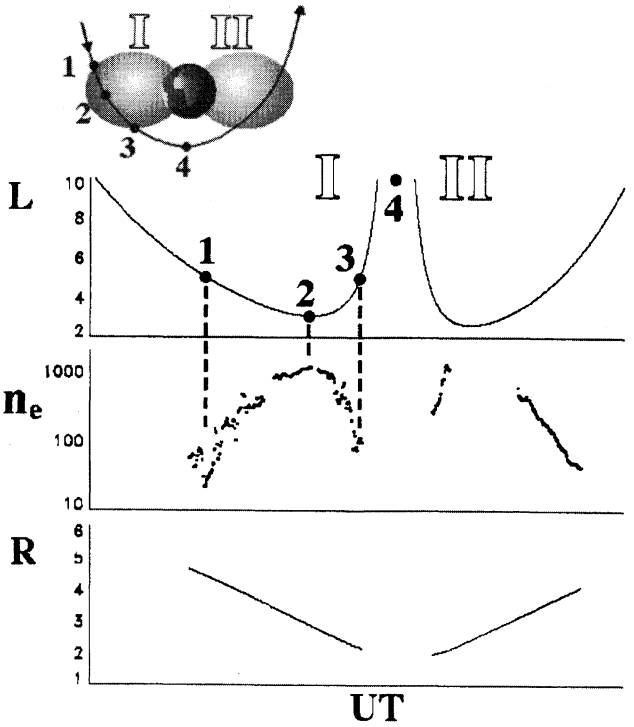

Figure 1. Sketch showing four points along the Polar spacecraft orbit and plots of L shell, electron density n_e, and radial distance from the Earth R for this orbit.

We assume a standard power law form with respect to R for the electron density on the outer part of the field line [e.g., *Radoski and Carovillano*, 1966]:

$$n_e = n_{e0} \left(\frac{LR_E}{R} \right)^{\alpha}, \tag{1}$$

where n_{e0} is the electron density at the equator. We can then calculate the α value for the field line containing points 1 and 3 as

$$\alpha = -\frac{\ln(n_{e1}/n_{e3})}{\ln(R_1/R_3)}, \tag{2}$$

where the subscripts "1" and "3" indicate values at points 1 and 3 in Figure 1. Note that we will use a slightly more complicated formula for the data analysis.

Attaining the field line density dependence through the method we have just described has its own unique problems. Equation (2) calculates the field line dependence as if points 1 and 3 were on the same flux tube, as if the densities were measured at those points at the same time, and as if a smooth density dependence exists along the flux tube. We do not know precisely that the two points are on field lines with the same equatorial radius, and this leads to error (which we will estimate as discussed in section 2). However, even if the equatorial radius of the field lines is the same (the fact that the points are on field lines with approximately the same equatorial radius is a key advantage over the method

used with the DE 1 data), the density at these points is sampled at different universal time (UT) and magnetic local time (MLT) (this is discussed further in section 2). Temporal variations (< 2-hour timescale; these could include short-timescale refilling structures), spatial fluctuations along the field line, azimuthal structure, and radial motion of the plasma observed at point 1 can all lead to decorrelation with the plasma observed at point 3 and thus to error in α as calculated using (2). Any specific value of α measured with two measurements of n_e should be considered questionable. Nevertheless, we expect that the statistical average of α from a large set of measurements will give us at least a rough idea of the typical field line density dependence, and that our results will be a useful complement to those attained from the DE 1 observations.

An outline of our paper is as follows: In section 2 we discuss the measurement of n_e, our data set, and our method of analysis to derive α values. In section 3 we discuss our results, and in section 4 we summarize our findings.

2. Data and Method

The electron density values used in this paper are obtained using the Polar Plasma Wave Instrument (PWI) [*Gurnett et al.*, 1995], which was in operation from March of 1996 to September of 1997. Inside the plasmasphere, where the electron plasma frequency f_{pe} is generally greater than the electron cyclotron frequency f_{ce}, it is typical to observe intense noise bands between f_{pe} and the upper hybrid resonance (UHR) frequency $f_{\rm UHR} = \sqrt{f_{pe}^2 + f_{ce}^2}$ [*Mosier et al.*, 1973; *Carpenter et al.*, 1981]. In the Polar data the UHR is often observed as a relatively narrowband emission poleward of and within the plasmasphere. The UHR frequency is obtained from the PWI and converted to a number density using

$$f_{pe}^2 = f_{\rm UHR}^2 - f_{ce}^2, \quad (3)$$

$$n_e(\mathrm{cm}^{-3}) \approx f_{pe}^2/(8980\ \mathrm{Hz})^2. \quad (4)$$

Two effects lead to a reduction in the total amount of UHR data available. First, the intensity of the noise bands is greatly reduced when Polar's trajectory is outside the plasmasphere and away from the equator, where the condition $f_{pe} \gg f_{ce}$ is often not satisfied. Second, at the lowest L values, when Polar penetrates deepest into the high-density plasmasphere, the preamplifiers located in the electric field antenna spheres often oscillate with a broadband signal centered near the UHR frequency, which obscures the natural UHR signal. The oscillations have recently been analyzed by *Kolesnikova and Beghin* [1999, 2001]. On the basis of these studies it may be possible in the future to recover the approximate plasma frequency from the fundamental oscillation frequency; however, for the time being these data have not been analyzed.

Values of the McIlwain parameter L [*McIlwain*, 1961] and MLT based on the International Geomagnetic Reference Field (IGRF) magnetic field model [*IAGA Division V Working Group 8*, 1991] were provided by the Polar spacecraft science data team [*Mish et al.*, 1995]. Note that LR_E is not precisely equal to the equatorial radius of a field line [*McIlwain*, 1961]. However, for the radii sampled in this study $R \gtrsim 2\ R_E$, it is approximately the radial distance in the equatorial plane of a dipole field line passing through the point of observation. As was mentioned in section 1, we obtain a density power law index by matching density measurements corresponding to the same L but different R (for example, points 1 and 3 in the sketch of Figure 1). In order to do this, the data for a particular pass through the plasmasphere are divided into two sections, one preceding the time when the spacecraft reaches its lowest L value (data from point 1 to point 2 in Figure 1) and one for times following (data from point 2 to point 3 in Figure 1). The range of L values sampled in both sets of data is typically divided into 50 bins (leading to a typical resolution in L of ~ 0.07), and density values in each bin are averaged.

Figure 2 shows density data for a randomly selected event in our data set. The electron density n_e is plotted versus radius R and L. Points 1–3 in Figure 2 correspond to the points with the same labels in Figure 1. As can be seen from the bottom panel of Figure 2, for most of the range of L shell sampled ($3.4 \le L \le 4.5$) the binned value with larger density is on the inner radius section, which indicates that the value of α in (1) is positive. However, for $4.5 \le L \le 4.75$ the opposite is true, indicating that $\alpha < 0$.

Taking each pair of density measurements with the same L value, we could use (2) to get an α value for the field line (where the subscript 1 (subscript 3) in equation (2) refers to a point on the segment 1–2 (2–3)). However, we would like to make a correction to partially compensate for the fact that our L values were based on the IGRF field. In order to do this, we map dipole field locations with R and L corresponding to the spacecraft position out to the equatorial radius using the T89c magnetic field model [*Tsyganenko*, 1989] with $K_p = 2$ (an average value for the time period of our data set) and no dipole tilt, and we determine the ratio L_1/L_3, where L_1 and L_3 are now the equatorial radii (different in general) based on the T89c field. (Actually, we mapped the field out for some sample L, R, and MLT values, and we interpolated the results to our data values.) Assuming that the density varies like

$$n_e = n_{e0}\left(\frac{L_0}{L}\right)^{\beta}\left(\frac{LR_E}{R}\right)^{\alpha} = n_{e0}\left(\frac{L_0}{L}\right)^{\beta}\bar{R}^{-\alpha}, \quad (5)$$

where $\bar{R} = R/(LR_E)$ and L_0 is a constant, we get

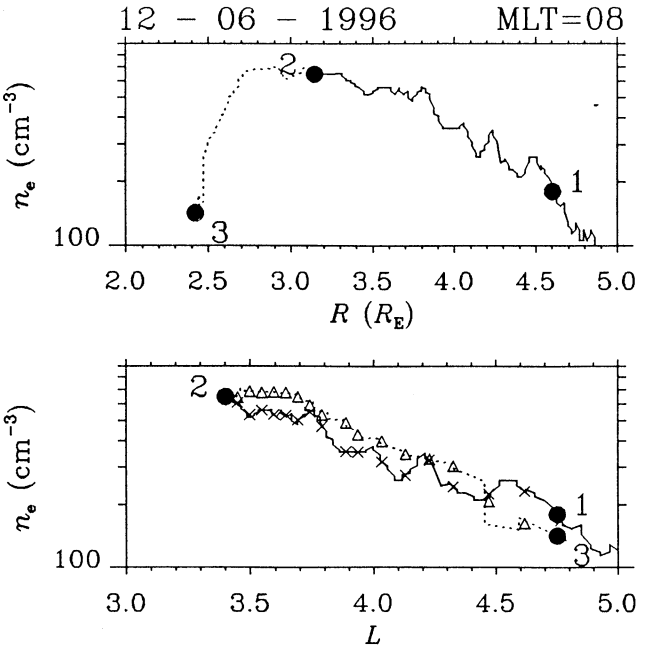

Figure 2. Electron density n_e versus (top) radius R and (bottom) L. Data are for a Polar satellite pass through the plasmasphere on December 6, 1996. The solid (dashed) curves show the outer (inner) radius sampling of L shells, and the crosses (diamonds) indicate the binned values used in the analysis of the data.

$$\alpha = -\frac{\ln(n_{e1}/n_{e3}) + \beta \ln(L_1/L_3)}{\ln(\bar{R}_1/\bar{R}_3)}, \qquad (6)$$

which takes into account the L correction. Furthermore, we take the β-dependent term in (6) as an estimate for the error in α due to uncertainty in the L value,

$$\Delta\alpha_L = \frac{\beta \ln(L_1/L_3)}{\ln(\bar{R}_1/\bar{R}_3)}. \qquad (7)$$

Equation (7) is a very rough estimate for error; the assumption is that the difference between the T89c magnetic field and the real field is less than the difference between the T89c field and a dipole field. The values of $\Delta\alpha_L$ are largest for large $L \gtrsim 5$ and nighttime local times for which the magnetic field has its greatest departure from a dipole field.

In order to use (6), we need to calculate

$$\beta = -\left.\frac{d\ln(n_e)}{d\ln(L)}\right|_{\bar{R}\ \text{const}}. \qquad (8)$$

We evaluate this by a finite difference of the unbinned densities on the inner radius section (because it is farther away from the equatorial radius). The resulting β values are then collected in the L bins and averaged. There is a subtlety involved in how we implement (8). The densities which are differenced to calculate the derivative in (8) must be evaluated at the same $\bar{R}$. We can adjust the density values within a certain L bin so they correspond to points with the same $\bar{R}$ value (the average value in the bin) before differencing. We do this using α in (1) (which represents the radial dependence in equation (5)), but the problem is that we need β to get α. We get around this problem by using an iterative solution for α. We first solve (6) for α assuming $\beta = 0$. With this value of α, we adjust the density values in the inner radius bin so that $\bar{R}$ is constant, finite difference the density values to get β (using equation (8)), and recalculate α using equation (6). We repeat these steps as necessary; the method converges rapidly in two or three iterations.

The time intervals selected for our analysis are listed in Table 1. There are 56 such intervals within the year May 27, 1996, to May 26, 1997, roughly one interval per week. Each time interval includes two passes through the plasmasphere on opposite sides of the Earth as illus-

Table 1. Time intervals for Data in Survey

Date	UT Interval	Date	UT Interval	Date	UT Interval
June 07, 1996	0900-1500	Oct. 04, 1996	1500-2000	Feb. 15, 1997	0400-1000
June 15, 1996	0800-1700	Oct. 11, 1996	0500-1000	Feb. 15, 1997	2200-0200
June 21, 1996	0700-1300	Oct. 17, 1996	0200-0700	Feb. 21, 1997	0100-0600
July 05, 1996	0400-1000	Oct. 25, 1996	0400-0800	Feb. 28, 1997	1000-1400
July 05, 1996	2200-0400	Oct. 25, 1996	2100-0000	March 07, 1997	0000-0500
July 12, 1996	1200-1800	Nov. 01, 1996	1200-1700	March 07, 1997	1800-2200
July 19, 1996	0200-0700	Nov. 08, 1996	0200-0500	March 14, 1997	0800-1300
July 19, 1996	2000-0100	Nov. 15, 1996	1000-1500	March 21, 1997	1600-2200
Aug. 02, 1996	0000-0300	Nov. 29, 1996	1000-1400	March 28, 1997	0700-1300
Aug. 02, 1996	1700-2300	Dec. 06, 1996	0000-0500	April 04, 1997	1500-2000
Aug. 10, 1996	0100-0600	Dec. 06, 1996	1700-2200	April 10, 1997	1200-1600
Aug. 10, 1996	1900-0000	Dec. 13, 1996	0800-1300	April 18, 1997	1400-1600
Aug. 17, 1996	0800-1300	Dec. 27, 1996	0600-1200	April 25, 1997	0600-1000
Aug. 29, 1996	0100-0600	Jan. 03, 1997	1500-2000	May 02, 1997	1400-1800
Aug. 29, 1996	1900-0000	Jan. 17, 1997	1300-1900	May 09, 1997	0600-1100
Sept. 05, 1996	0900-1500	Jan. 24, 1997	0400-1000	May 16, 1997	1500-1900
Sept. 13, 1996	1000-1500	Jan. 31, 1997	1200-1700	May 23, 1997	0600-1000
Sept. 20, 1996	0000-0500	Feb. 07, 1997	0300-0800	May 29, 1997	0300-0900
Sept. 20, 1996	1900-2300	Feb. 07, 1997	2000-0200		

trated in Figure 1. All together, there were 908 pairs of density measurements. We screened our data with several different criteria. First we eliminated pairs of points with a difference in $R < 0.2\ R_E$, since in that case, (6) leads to uncharacteristically large values of $|\alpha|$ for a particular L shell. (We need a large enough difference in R to eliminate the effect of temporal fluctuations in n_e.) Binned data with data points for which the unbinned data had $d\log_{10}(n_e)/dL > 1$ and binned densities for which β (equation (8)) varied by more than two standard deviations from the mean value for the entire data set were not used; a visual check revealed that these criteria eliminated all the data which appeared to have unacceptable spatial or temporal fluctuations. A visual check was made for passes in which the densities on the inner and outer sections were clearly uncorrelated (one might have had a plasmapause while the other did not), and these were eliminated from the data set. Finally, values of α more than two standard deviations away from the mean were dropped. (This had little effect on the averages since the error bars on these points were large, but it cleaned up the plots since these points are outliers.)

After applying the screening criteria, the end result is that the number of paired densities is reduced to 555. For each of these we found a value of α using (6). The sampled L values ranged from 2.5 to 6.3. It should be remembered that we are only measuring the radial density dependence along field lines up to the latitudes sampled by Polar and for which Polar is able to obtain reliable density measurements; this corresponds roughly to $R \gtrsim 2\ R_E$. In Figure 3 we plot the change in MLT, ΔMLT in hours, versus the change in UT, ΔUT in hours, between the two measurements in each pair.

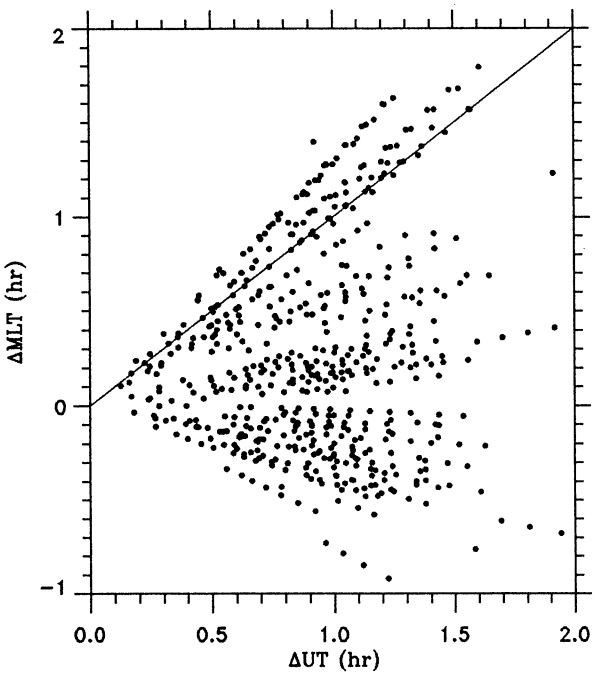

Figure 3. Change in MLT, ΔMLT, versus change in UT, ΔUT, between the two measurements in each pair of observations corresponding to the same L shell.

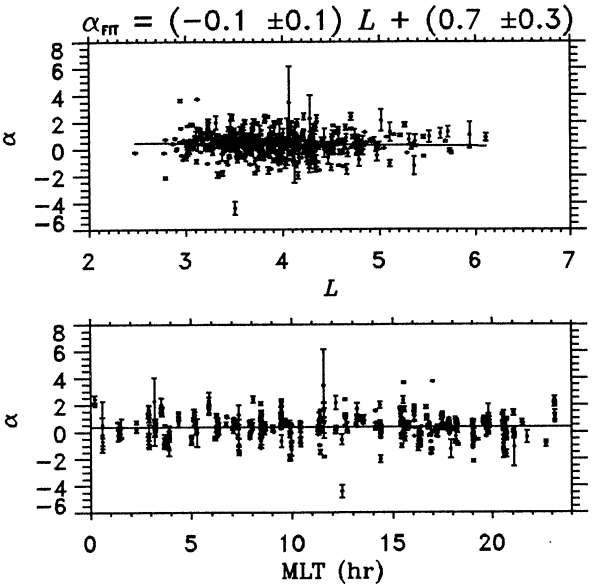

Figure 4. Scatterplot of the density power law index α versus (top) L and (bottom) MLT. Data are for pairs of density observations in our plasmaspheric data set (electron density $n_e \geq 100\ \mathrm{cm}^{-3}$). The solid curve in the top panel is a linear least squares fit with the fit parameters given above the plot; the solid curve in the bottom panel is drawn at the average value of $\alpha = 0.37 \pm 0.8$.

In this paper we will use all these points for our statistical calculations; however, we note that one might (especially with a larger data set) look at the set of data with ΔMLT $\simeq$ ΔUT. For this set one would be approximately looking at the same flux tube if it corotates with the Earth.

3. Results

Figures 4 and 5 represent the results of our study. For each pair of density measurements, we calculate the average of the two measurements. The total data set is divided into two groups with this average electron density n_e greater than or less than 100 cm^{-3}. We loosely consider the group with $n_e \geq 100\ \mathrm{cm}^{-3}$ ($< 100\ \mathrm{cm}^{-3}$) to be plasmaspheric (plasma trough) data. There are 501 (54) pairs of measurements in the plasmaspheric (plasma trough) data set. Figures 4 and 5 are scatterplots of the density power law index α versus L and versus MLT for the plasmaspheric and plasma trough data, respectively. The error bars displayed represent the estimate for the error in α, $\Delta\alpha_L$ (equation (7)), due to the uncertainty in measuring L.

The best linear fit parameters for α versus L are shown above Figures 4 and 5. In order to calculate the fit parameters and average values given below, we used an error for each point i, $\Delta\alpha_i$, found by adding in quadrature the error in α attributed to uncertainty in L, $\Delta\alpha_{Li}$ (equation (7)), to the standard deviation of the α_i measurements ($\sqrt{\sum_i(\alpha_i - <\alpha>)^2/(N-2)}$, where N is the number of measurements in the plasmaspheric or plasma trough data set and $<\alpha> = \sum_i(\alpha_i)/N$).

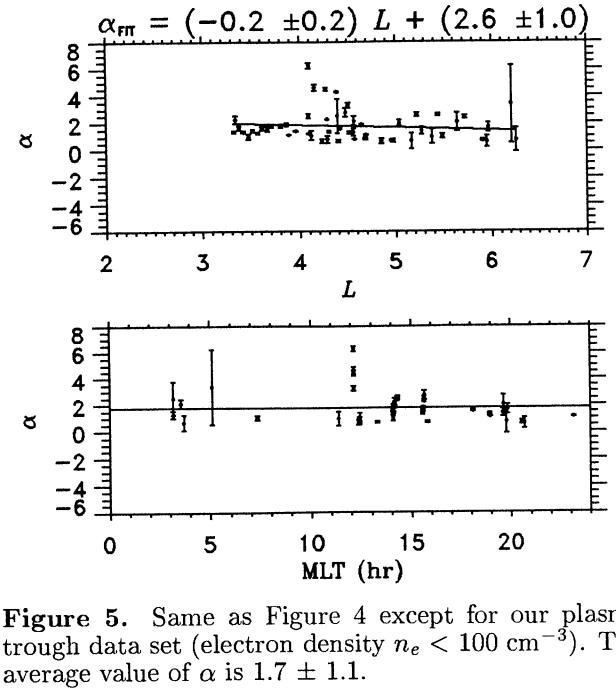

Figure 5. Same as Figure 4 except for our plasma trough data set (electron density $n_e < 100$ cm^{-3}). The average value of α is 1.7 ± 1.1.

The standard deviation of the inferred α values is an upper limit for unknown errors (some of the variation in inferred α values should result from real variation in the actual α). The fits for α versus L were then found using a linear least squares fit with errors [*Bevington and Robinson*, 1992]. There is a slight negative correlation between L and α discernible in Figures 4 and 5; however, considering its error, the slope could be nearly zero. There is no clear dependence with respect to MLT in either data set.

The average value of α is determined using the formula $\sum_i(\alpha_i/\Delta\alpha_i^2)/\sum_i(1/\Delta\alpha_i^2)$, and its error is found from $\sqrt{\sum_i[(\alpha_i - <\alpha>)^2/\Delta\alpha_i^2]/\sum_i(1/\Delta\alpha_i^2)}$. The average value of α for the plasmaspheric data is 0.37±0.8, while the average value of α for the plasma trough data is 1.7 ± 1.1. The average value of α for the entire data set is 0.50±1.0. Thus the average for our plasmaspheric data set, $\alpha = 0.37 \sim 0$, is consistent with the DE 1 results [*Gallagher et al.*, 2000] and the whistler results [*Angerami and Carpenter*, 1966]. The $\alpha = 1.7 \pm 1.1$ result in the plasma trough may imply (but note the large error) a steeper density dependence than that of the DE 1 data (see section 1 for a discussion of the DE 1 data), but this result also implies a milder radial dependence than the collisionless $\alpha = 4$ found by *Angerami and Carpenter* [1966]. Besides the fact that the ULF wave studies measure mass density dependence rather than electron density dependence, there are too few ULF wave results to make any firm comparison, but our average values for α are certainly within the range of values found by *Takahashi and McPherron* [1982] and *Menk et al.* [1999].

For diffusive equilibrium we estimate the density scale height (neglecting the electric potential) as $k(T_p + T_e)/(m_p g \sin(\theta_{\rm dip}))$, where k is the Boltzmann constant; T_p and T_e are the proton and electron temperatures, respectively; m_p is the proton mass; $g = g_E R_E^2/R^2$ and g_E are the gravitational acceleration at radius R and at the Earth's surface, respectively; and $\theta_{\rm dip}$ is the dipole tilt angle, the angle between the horizontal and the direction of the magnetic field (P. Richards, private communication, 2000). Taking as an example $R = 3.5\ R_E$ on an $L = 4$ dipole field line, and $T_p = T_e = 5500$ K, we find a scale height of 24 R_E. Assuming (1), the density scale height is $|n_e/(dn_e/dR)| = R/\alpha$, which is equal to 24 R_E for $\alpha = 0.15$. This value is not far from our average plasmaspheric value 0.37 ± 0.8. Results from the field line interhemispheric plasma (FLIP) model [*Torr et al.*, 1990; *Craven et al.*, 1995] indicate that the high-altitude density gradient along field lines is small, $\alpha \sim 0$, regardless of L or MLT for the range of L studied here ($2.5 \leq L \leq 6.3$) (P. Richards, private communication, 2000). Since the low-density plasma trough is thought to be to a certain extent collisionless, it might make sense to expect the collisionless result $\alpha = 4$ [*Lemaire and Gringauz*, 1998, and references therein] or perhaps $\alpha = 3$ for flux coming up a flux tube (constant number of particles crossing a unit cross-sectional area of a flux tube, $\propto B^{-3}$, per unit time) (P. Richards, private communication, 2000). Our plasma trough result ($\alpha = 1.7 \pm 1.1$) is in between these kinetic results and the diffusive equilibrium $\alpha \sim 0$.

4. Conclusions

Using electron density measurements based on the measurement of the upper hybrid resonance frequency by the Polar PWI instrument, we have examined the radial density dependence along field lines in and near the plasmasphere. Our technique depends on the fact that the Polar spacecraft crosses particular L values at two different points with different radial distance R (Figure 1). Sample L values range from 2.5 to 6.3. It is important to emphasize that the density dependence we are measuring is characteristic of the outer part of the plasmaspheric field lines that Polar samples. Characteristically, the sampled R values are greater than 2.0 R_E.

In our outer plasmaspheric data set ($n_e \geq 100$ cm^{-3}) we find that, on average, the density is flat along field lines (within the uncertainty of our measurements) up to the latitudes sampled by Polar. In the plasma trough data set ($n_e < 100$ cm^{-3}) there is, on average, a mild radial dependence, $n_e \propto R^{-1.7}$. There is a very slight trend perceptible in both data sets toward flatter density at larger L values (see Figures 4 and 5). There is no clear trend with respect to MLT in either data set.

A possibly surprising result of our study is that the distribution of density power law index is not very broad (standard deviation of 0.8 and 1.1 for plasmasphere and plasma trough, respectively). As mentioned in section 1, our method has the disadvantage that the two density observations used for determining the field line

radial density dependence are measured at different UT and MLT (Figure 3). In addition, there is no guarantee that one of our density measurements does not result from a fluctuation along a field line. We expect that these effects will lead to a broadening of the distribution of inferred density power law index α (equation (1)). Thus the distribution of α values characteristic of the real magnetosphere might be even less than the values we have found.

Acknowledgments. We are grateful to Iowa PWI team, including D. Gurnett and J. Pickett for supplying the upper hybrid resonance data (supported by NASA contract NAS5-30371 and grant NAG5-7943); we thank J. Pickett for answering our questions about the data. We are also grateful to the Polar spacecraft science data team for supplying spacecraft ephemeris data, to J. Vernetti and W. Teitler, who supplied us with CD-ROMs containing the data (supported by NASA grant NAG5-3182), and to W. Mish for answering our questions about the data. We also thank Jim LaBelle, Paul Craven, and Phil Richards for helpful discussions. Work at Dartmouth was supported by NASA grants NGT5-50153 and NAG5-7442 and NSF grant ATM-9911975. Work at the University of Iowa was supported by subcontract 14280500 to MSFC/NASA project NAG8-1153.

Janet G. Luhmann thanks the referees for their assistance in evaluating this paper.

References

Angerami, J.J., and D.L. Carpenter, Whistler studies of the plasmapause in the magnetosphere, 2, Electron density and total tube electron content near the knee in magnetospheric ionization, *J. Geophys. Res.*, *71*, 711, 1966.

Bevington, P.R., and D.K. Robinson, *Data Reduction and Error Analysis for the Physical Sciences*, pp. 96-114, McGraw-Hill, New York, 1992.

Carpenter, D.L., and R.R. Anderson, An ISEE/whistler model of equatorial electron density in the magnetosphere, *J. Geophys. Res.*, *97*, 1097, 1992.

Carpenter, D.L., R.R. Anderson, T.F. Bell, and T.R. Miller, A comparison of equatorial electron densities measured by whistlers and by a satellite radio technique, *Geophys. Res. Lett.*, *8*, 1107, 1981.

Chan, A.A., M. Xia, and L. Chen, Anisotropic Alfvén-ballooning modes in Earth's magnetosphere, *J. Geophys. Res.*, *99*, 17,351, 1994.

Craven, P.D., R.H. Comfort, P.G. Richards, and J. Grebowsky, Comparisons of modeled N+, O+, H+, and He+ in the midlatitude ionosphere with mean densities and temperatures from Atmospheric Explorer, *J. Geophys. Res.*, *100*, 257, 1995.

Craven, P.D., D.L. Gallagher, and R.H. Comfort, Relative concentration of He^+ in the inner magnetosphere as observed by the DE 1 retarding ion mass spectrometer, *J. Geophys. Res.*, *102*, 2279, 1997.

Décréau, P.M.E., D. Carpenter, C.R. Chappell, R.H. Comfort, J. Green, R.C. Olsen, and J.H. Waite Jr., Latitudinal plasma distribution in the dusk plasmaspheric bulge: Refilling phase and quasi-equilibrium state, *J. Geophys. Res.*, *91*, 6929, 1986.

Gallagher, D.L., P.D. Craven, and R.H. Comfort, Global core plasma model, *J. Geophys. Res.*, *105*, 18,819, 2000.

Gurnett, D.A., et al., The Polar Plasma Wave Instrument, *Space Sci. Rev.*, *71*, 583, 1995.

IAGA Division V Working Group 8, International geophysical reference field, *J. Geomagn. Geoelectr.*, *43*, 1007, 1991.

Kolesnikova, E., and C. Beghin, The instability problem of the electric antennas on the Polar and Cluster-1 types near the plasma resonances, *Internal Rep. LPCE/NTS/065.B*, Lab. de Phys. et Chim. de L'Environ., Orleans, France, Sept., 1999.

Kolesnikova, E., and C. Beghin, The instability problem of the electric field antennas on the Polar spacecraft, *Radio Sci.*, in press, 2001.

Lemaire, J.F., and K.I. Gringauz, *The Earth's Plasmasphere*, pp. 222-249, Cambridge Univ. Press, New York, 1998.

McIlwain, C.E., Coordinates for mapping the distribution of magnetically trapped particles, *J. Geophys. Res.*, *66*, 3681, 1961.

Menk, F.W., D. Orr, M.A. Clilverd, A.J. Smith, C.L. Waters, D.K. Milling, and B.J. Fraser, Monitoring spatial and temporal variations in the dayside plasmasphere using geomagnetic field line resonances, *J. Geophys. Res.*, *104*, 19,955, 1999.

Mish, W.H., J.L. Green, M.G. Reph, and M. Peredo, ISTP science data systems and products, *Space Sci. Rev.*, *71*, 815, 1995.

Mosier, S.R., M.L. Kaiser, and L.W. Brown, Observations of noise bands associated with the upper hybrid resonance by the IMP 6 radio astronomy experiment, *J. Geophys. Res.*, *78*, 1673, 1973.

Olsen, R.C., The density minimum at the Earth's magnetic equator, *J. Geophys. Res.*, *97*, 1135, 1992.

Olsen, R.C., S.D. Shawhan, D.L. Gallagher, J.L. Green, C.R. Chappell, and R.R. Anderson, Plasma observations at the Earth's magnetic equator, *J. Geophys. Res.*, *92*, 2385, 1987.

Poulter, E.M., W. Allan, and G.J. Bailey, ULF pulsation eigenperiods within the plasmasphere, *Planet. Space Sci.*, *36*, 185, 1988.

Price, I.A., C.L. Waters, F.W. Menk, G.J. Bailey, and B.J. Fraser, A technique to investigate plasma mass density in the topside ionosphere using ULF waves, *J. Geophys. Res.*, *104*, 12,723, 1999.

Radoski, H.R., and R.L. Carovillano, Axisymmetric plasmasphere resonances: Toroidal mode, *Phys. Fluids*, *9*, 285, 1966.

Takahashi, K., and R.L. McPherron, Harmonic structure of Pc 3-4 pulsations, *J. Geophys. Res.*, *87*, 1504, 1982.

Torr, M.R., D.G. Torr, P.G. Richards, and S.P. Yung, Mid- and low-latitude model of thermosphere emissions, 1, O+(2*P*) 7320 and N2(2*P*) 3371, *J. Geophys. Res.*, *95*, 147, 1990.

Tsyganenko, N.A., A magnetospheric magnetic field model with a warped tail current sheet, *Planet. Space Sci.*, *37*, 5, 1989.

Young, E.R., D.G. Torr, P. Richards, and A.F. Nagy, A computer simulation of the midlatitude plasmasphere and ionosphere, *Planet. Space Sci.*, *28*, 881, 1980.

R. E. Denton, M. K. Hudson, E. G. Miftakhova, and S. L. Young, Department of Physics and Astronomy, 6127 Wilder Laboratory, Dartmouth College, Hanover, NH 03755 (richard.denton@dartmouth.edu)

D. L. Gallagher, NASA Marshall Space Flight Center, Mail Code ES83, Building 4481, Room 382, Huntsville, AL 35812 (dennis.gallagher@msfc.nasa.gov)

J. Goldstein, Department of Physics and Astronomy, MS-108, 6100 Main Street, Rice University, Houston, TX 77005-1892 (jerru@hydra.rice.edu)

J. D. Menietti, Department of Physics and Astronomy, University of Iowa, Iowa City, IA 52242 (jdm@space.physics.uiowa.edu)

(Received March 1, 2000; revised November 8, 2000; accepted November 9, 2000.)